PET of Hypoxia: Current and Future Perspectives

Sean Carlin[1] and John L. Humm[2]

[1]Radiochemistry and Imaging Sciences Service, Department of Radiology, Memorial Sloan-Kettering Cancer Center, New York, New York; and [2]Department of Medical Physics, Memorial Sloan-Kettering Cancer Center, New York, New York

In the past 25 y, a large amount of clinical experience with hypoxia PET tracers has accumulated. This article discusses recent improvements in image acquisition protocols and tracer pharmacology that have resulted in improved understanding of the underlying physiologic processes. The widespread clinical adoption of hypoxia PET tracers will depend largely on their utility in treatment prescription and in outcome monitoring. The establishment and validation of hypoxia-directed treatment protocols are still under development, and it is envisaged that the design and use of future hypoxia PET tracers will develop as part of this process.

Key Words: hypoxia; PET; 2′-nitroimidazole; ^{64}Cu-ATSM; ^{18}F-fluoromisonidazole

J Nucl Med 2012; 53:1171–1174
DOI: 10.2967/jnumed.111.099770

Currently, nuclear imaging techniques, particularly PET, are best poised to perform quantitative estimates of tumor hypoxia, because of the availability of several radiotracers that become selectively entrapped within regions of tissue hypoxia. Most of these radiotracers are from the family of 2′-nitroimidazoles (*1*), although alternative hypoxia radiotracers are also available.

The first group to propose the noninvasive imaging of hypoxia by PET was Janet Rasey and her colleagues at the University of Washington. These investigators pioneered the synthesis of ^{18}F-fluoromisonidazole and subsequently demonstrated the feasibility of ^{18}F-fluoromisonidazole PET for imaging the hypoxic fractions of a variety of tumors in humans. After intravenous injection, ^{18}F-fluoromisonidazole clears from the blood compartment relatively slowly and traverses tissue by passive diffusion. Because of these characteristics, PET protocols require imaging between 2 and 3 h after injection.

ANALYSIS OF HYPOXIA PET IMAGES

Analysis of the pixel variation within normal tissues in these studies has led to an operational definition that activity concentrations greater than 1.3 or 1.4 times the concentration in blood reflect locoregional hypoxia. An early clinical study using ^{18}F-fluoromisonidazole in a diverse range of tumor types found that, using this criterion to define hypoxia, 36 of 37 contained a measurable fractional hypoxic volume (*2*). An important caveat associated with these low tumor-to-blood ratios is that they are not entirely unexpected. In vitro experiments show that the uptake of ^{18}F-fluoromisonidazole in cells under hypoxic (0.5% O_2) versus normoxic (21% O_2) conditions is typically about 6:1. Thus a subtumor region containing 100% hypoxic tissue could theoretically produce a signal 6-fold higher than a normoxic region. However, histologic analysis shows that the hypoxia exists as patches or ribbons dispersed through the disease. These staining patterns suggest that individual PET voxels consist of far less than 100% hypoxic elements—typically 5%–30%. Thus, ^{18}F-fluoromisonidazole uptake within a hypoxic tumor voxel consisting of 20% hypoxia plus 80% normoxic tissue would not be expected to yield a ratio of 6:1 but only 2:1 ($0.2 \times 6 + 0.8 \times 1 = 2.0$). By comparison, the large uptake ratio between tumor and muscle seen with ^{18}F-FDG is a consequence of every tumor cell, rather than a fraction, exhibiting facilitated uptake and entrapment. A visual representation is shown in Figure 1.

The low signal ratios between normoxic and hypoxic tumor locations are also a consequence of partial-volume averaging, giving rise to statistical uncertainties associated with image-based measurements. Nehmeh et al. (*3*) performed repeated baseline ^{18}F-fluoromisonidazole PET/CT examinations in immobilized head and neck cancer patients for which accurate registration was possible. The 2 studies, performed 3 d apart, were designed to verify the constancy of hypoxia distribution over the duration required to generate a head and neck radiotherapy plan and begin treatment. Statistical analysis of the voxel variability of the ^{18}F-fluoromisonidazole signal intensity at corresponding image locations between 2 PET baseline scans showed significant image variability. Whereas such variability can also be a consequence of spatial shifts in acute hypoxia, the poor count-to-noise ratio of late ^{18}F-fluoromisonidazole hypoxia PET images is a concern for the clinical use of the spatial information within these images for radiotherapy planning purposes. This problem is not unique to ^{18}F-fluoromisonidazole, however, and represents a significant challenge to any radiotracer that attempts to identify a tumor subregion or a specific subset of cells within the tumor.

Received May 2, 2012; revision accepted Jul. 9, 2012.
For correspondence or reprints contact: Sean Carlin, Department of Radiology, MSKCC, 1275 York Ave., New York, NY, 10021.
E-mail: carlins@mskcc.org
Published online Jul. 12, 2012.

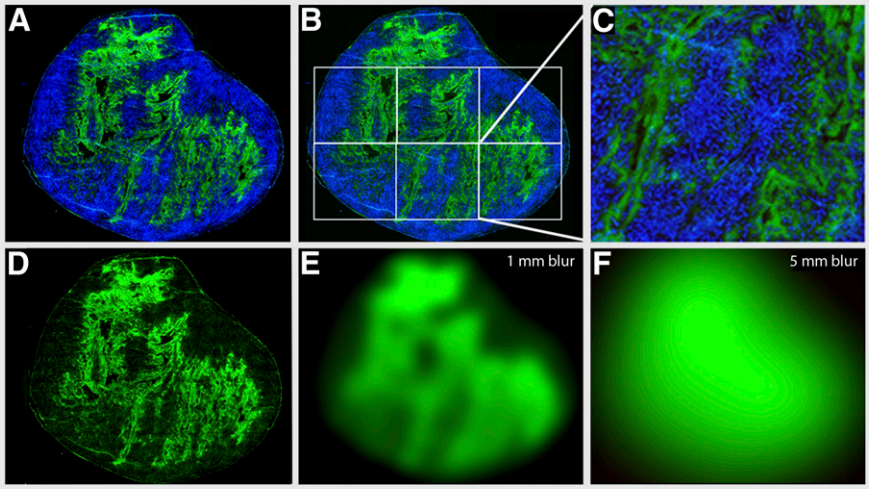

FIGURE 1. (A) Histologic tumor section indicating hypoxia tracer pimonidazole (green) and vascular perfusion marker Hoechst 33342 (blue). (B) Same image with six 5-mm^2 areas superimposed, representing approximate resolution of a clinical PET scanner. (C) Single 5-mm^2 region at high magnification, containing approximately 20% pimonidazole-positive area. (D–F) Same pimonidazole distribution, but with a gaussian blur of 1 mm (E) and 5 mm (F) applied. This series demonstrates that PET voxel values are a function of both maximal uptake of tracer and hypoxic fraction of voxel. Averaging signal results in lowering overall tumor-to-blood ratios for hypoxia tracers. Increasing PET spatial resolution (E vs. F) would result in improved visualization of regions with higher tumor-to-blood ratios.

DYNAMIC HYPOXIA PET

The limitations in defining hypoxia from late single-time-point ^{18}F-fluoromisonidazole PET images might be overcome using a kinetic modeling approach in which the rate of irreversible tracer trapping derived from a dynamic imaging series is used as the quantitative measure for each tumor subregion. An example of such a dynamic dataset is shown in Figure 2. This approach was first implemented in clinical studies by Thorwarth et al. at Tübingen University (*4*) and demonstrated the importance of kinetic analysis to separate the PET signal component associated with hypoxia-specific radiotracer binding from signal associated with unbound freely diffusible tracer.

One difficulty of performing voxelwise compartmental analysis is the statistical uncertainty associated with PET data from a single voxel. These uncertainties were studied by Wang et al. (*5*) using simulated PET datasets and the Philips Voxulus compartmental analysis toolkit. One thousand simulated dynamic scans of a phantom within inserted regions exhibiting hypoxic and necrotic tissue characteristics and noise characteristics representative of actual patient dynamic PET scans were generated for compartmental analysis. At a 15% image noise level, the ^{18}F-misonidazole-trapping rate constant (k_3) exhibited an SD of 13.5%. This uncertainty is relatively large but can be reduced if the kinetic parameters are averaged over a multivoxel region of interest, albeit at the cost of decreased spatial resolution. Parametric maps of k_3, that is, images whose voxel intensity reflect a calculated irreversible trapping rate constant for that location, reflect a more reliable display of the intratumor variation of hypoxia than a PET image of the concentration of radiotracer at the time of image acquisition. This is especially important when considering interventions that might reduce blood flow, and consequently the delivery of the hypoxia imaging agent to the tumor, yet incur a transient increase in the amount of tumor hypoxia (*6*).

CURRENT CLINICAL HYPOXIA PET TRACERS

The 2′-nitroimidazole compounds exhibit a rate of uptake that is strictly dependent on the oxygen concentration, with the rate of accumulation increasing as partial pressure of oxygen (pO_2) falls below 10 mm Hg in most cases (*7*). This property has resulted in the synthesis of several fluorinated and iodinated agents that use the nitroimidazole basic structure. Of these, ^{18}F-fluoroazomycinarabinofuranoside (^{18}F-FAZA), and its iodinated counterpart (^{123}I/^{124}I-IAZA), are promising alternatives to ^{18}F-fluoromisonidazole. Head-to-head comparisons between ^{18}F-FAZA, ^{124}I-IAZA, and ^{18}F-fluoromisonidazole in preclinical animal studies imaged at

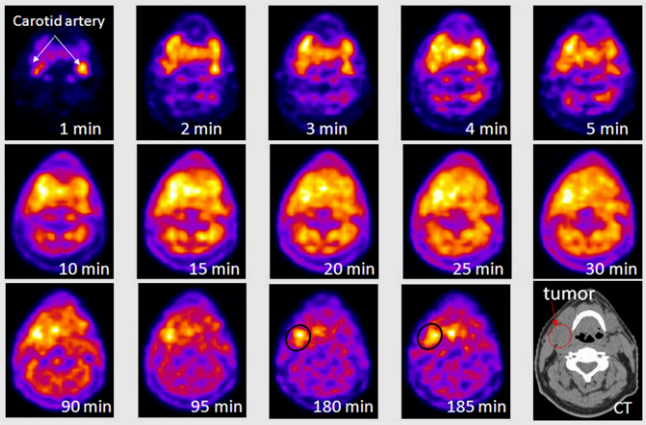

FIGURE 2. Results of a dynamic PET scan as a function of time after injection with ^{18}F-fluoromisonidazole. Single reconstructed PET slice is displayed through center of head and neck tumor. First 5 frames were of 1-min duration, followed by 5 frames of 5-min duration. At 30 min after injection, patient was removed from scanner and then reimaged at 90 min and 180 min after injection. Images were coregistered using low-dose CT scan (depicted in final image in series). This series shows evolution of ^{18}F-fluoromisonidazole distribution within patient from initial blood pool to selective sequestration within hypoxic tumor subvolume.

3 h after injection demonstrated faster vascular clearance of ^{18}F-FAZA, resulting in an increased tumor-to-blood ratio (5.19) relative to that for ^{18}F-fluoromisonidazole (3.98). ^{124}I-IAZA exhibited a slightly poorer tumor-to-blood ratio at 3 h after injection but allowed (on account of the longer physical half-life of the iodine isotopes) later-time-point imaging (*8*). More recent clinical studies have successfully evaluated the feasibility of ^{18}F-FAZA for imaging hypoxia in head and neck tumors, glioma, lymphoma, and lung (*9*).

A very different chemical class of hypoxia radiotracer that has been intensively investigated in both preclinical and clinical studies is the dithiosemicarbazone compounds. The potential of these agents for hypoxia imaging was first reported by Fujibayashi et al. from Eukui Medical School in Japan (*10*) and by Holland et al. from Washington University, St. Louis (*11*). The ability to rapidly label the precursor compound with a variety of copper isotopes of varying half-lives, including ^{60}Cu ($t_{1/2}$ = 23.7 min), ^{61}Cu ($t_{1/2}$ = 3.35 h), ^{62}Cu ($t_{1/2}$ = 9.74 min), and ^{64}Cu ($t_{1/2}$ = 12.7 h), provides this marker with tremendous flexibility.

One potential difficulty with copper-diacetyl-bis(*N*4-methylthiosemicarbazone) (ATSM) is the universality and reliability of its use as a hypoxia imaging agent among different tumor types. In vitro experiments examining ^{64}Cu-ATSM uptake have shown rapid but quite variable absolute uptakes among different cell lines at the same pO_2 (*12*), suggesting that the observed high uptake in tumors may only partly be a direct consequence of hypoxia (*13*). Nevertheless, extremely high-contrast images of copper-ATSM have been obtained in a variety of tumor sites, suggestive of significant tumor hypoxia (*11*). ACRIN trial 6682, assessing the utility of copper-ATSM as a biomarker of treatment outcome in cervical carcinoma, is currently under way. Whether hot spots within PET images of copper-ASTM represent hypoxia is unknown, but they do provoke further investigation into the uptake and retention mechanism of this radiotracer. It is possible that that pO_2 is only one of several mechanisms affecting copper-ATSM distribution and that copper-ATSM uptake might better represent a general prognosticator of poor treatment response than of tumor hypoxia per se. However, in this context the absolute uptake of ^{18}F-fluoromisonidazole is not purely pO_2-dependent but is also partially subject to changes in vascular delivery and cellular reductase expression (*6,14*).

HYPOXIA PET TRACERS: THE NEXT GENERATION

A wide range of fluorinated nitroimidazole compounds have previously been examined in an attempt to identify those with favorable whole-body clearance or more rapid pO_2-sensitive bioreduction. Early examples include metronidazole, etanidazole, EF1, EF3, and SR4454 (*15*). The primary determinant of the pharmacokinetics of each of these compounds is the octanol–water partition coefficient (logP). In general, the more lipophilic compounds (positive logP) display rapid tissue equilibration and higher first-pass tumor uptake rates but slower background clearance and higher liver activity. The hydrophilic compounds (negative logP) display the reverse characteristics: rapid renal clearance, lower liver uptake, and reduced production of metabolites, at the cost of lower absolute uptake and more heterogeneous tumor distribution. It is becoming increasingly apparent that a single hypoxia tracer is unlikely to be of optimal utility in every clinical situation and that particular disease characteristics will favor the use of a given hypoxia tracer–radioisotope combination (*14*). The newer generation of 2-nitroimidazole hypoxia tracers under clinical investigation seeks to exploit pharmacokinetic differences in ^{18}F-fluoromisonidazole and will—it is hoped—find specific roles in which these characteristics can be maximally exploited.

^{18}F-2-(2-Nitro-1H-Imidazol-1-yl)-*N*-(2,2,3,3,3-Pentafluoropropyl)-Acetamide (^{18}F-EF5)

The nitroimidazole EF5 has been extensively used for ex vivo immunohistochemical detection of bioreduced adducts, which indicate regions of tumor hypoxia. However, ^{18}F-EF5, first investigated as a hypoxia PET tracer in 2001, has only recently appeared in a clinical setting. In contrast to many of the second-generation hypoxia tracers, ^{18}F-EF5 has a high octanol–water partition coefficient (5.71, vs. 0.4 for fluoromisonidazole), resulting in greater cell membrane permeability and slower blood clearance (plasma half-life, 13 h) (*16*). As opposed to rapid clearance kinetics, this characteristic aims to exploit improved rates of tumor uptake and homogeneity of tracer distribution, which can present significant issues with the more hydrophilic nitroimidazole tracers (*6,9*). Radiofluorination of EF5 is more technically challenging than that of ^{18}F-fluoromisonidazole or ^{18}F-FAZA, but a recent description of a high-specific-activity synthesis method (*17*) is encouraging for the potentially wider adoption of this radiotracer.

^{18}F-3-Fluoro-2-(4-((2-Nitro-1H-Imidazol-1-yl)Methyl)-1H-1,2,3-Triazol-1-yl)Propan-1-ol (^{18}F-HX4)

^{18}F-HX4 is a next-generation 2-nitroimidazole tracer specifically designed to maximize pharmacokinetic and clearance properties. Initial studies in humans demonstrate rapid renal clearance and urinary excretion of ^{18}F-HX4, with a plasma half-life of approximately 3 h and an organ dosimetry profile similar to that of ^{18}F-fluoromisonidazole. Phase I studies in 6 patients (4 non–small cell lung carcinoma, 1 thymus carcinoma, and 1 colon carcinoma) recorded a median tumor-to-muscle ratio of 1.40 at 120 min after injection, although no attempt was made to determine the optimal imaging time points in that study (*18*). Subsequent studies using rodent models confirmed previous observations of reduced liver uptake and radiotracer metabolism when compared with ^{18}F-fluoromisonidazole and, most importantly, validated that tracer uptake was indeed oxygen-dependent. However, tumor-to-background ratios appeared similar to those reported for ^{18}F-fluoromisonidazole in studies using the same tumor model (*19*). Whether ^{18}F-HX4 provides any significant advantage over ^{18}F-fluoromisonidazole in a clinical setting remains to be determined.

^{18}F-Fluoroerythronitromidazole (^{18}F-FETNIM)

The hydrophilic nature of ^{18}F-FETNIM is assumed to be responsible for the observed rapid renal clearance and low liver uptake, compared with ^{18}F-fluoromisonidazole, and may also explain the counterintuitive positive correlation between tumor blood flow and initial tumor ^{18}F-FETNIM uptake (*20*). Recent clinical studies have indicated that high ^{18}F-FETNIM SUV may be predictive of treatment outcome in non–small cell lung and esophageal squamous cell tumors (*21,22*). However, as with ^{18}F-HX4, it is not clear whether the use of this tracer presents any advantages over current ^{18}F-fluoromisonidazole imaging protocols.

CLINICAL APPLICATIONS OF HYPOXIA IMAGING

The ability to determine the degree and extent of tumor hypoxia is important both as a prognostic biomarker (*23*) and as a means of selection of patients for hypoxia-directed therapies. The intratumor spatial distribution of hypoxia can potentially serve as a target in radiotherapy planning (*24*) and also indicate the use of a growing number of adjunct therapies (*25*). Of these, the current crop of hypoxia-activated nitroaromatic prodrugs such as TH-302 and PR-104 seems most likely to make a significant clinical impact. Because the activation of these compounds shares a similar mechanism with the bioreduction of the 2′-nitroimidazoles, there appears a rationale for the incorporation of hypoxia PET into the evaluation and implementation of these drugs in the clinic.

CONCLUSION

In the past 25 y, a large amount of clinical experience with hypoxia PET tracers has accumulated. Laboratory advances have allowed fine-tuning of the pharmacologic performance properties of these compounds, which, combined with improvements in PET camera technology and image acquisition protocols, have improved the understanding of the underlying physiologic processes. However, it is becoming increasingly apparent that the use of a single "best" hypoxia PET tracer in all circumstances may not yield either optimal or consistent results and that factors other than the underlying pO_2 may affect the tissue distribution and uptake of these tracers. The widespread clinical adoption of hypoxia PET tracers will depend largely on their utility in treatment prescription and in outcome monitoring. The establishment and validation of hypoxia-directed treatment protocols are still under development, and it is envisaged that the design and use of future hypoxia PET tracers will develop as part of this process.

ACKNOWLEDGMENT

No potential conflict of interest relevant to this article was reported.

REFERENCES

1. Chitneni SK, Palmer GM, Zalutsky MR, Dewhirst MW. Molecular imaging of hypoxia. *J Nucl Med.* 2011;52:165–168.
2. Rasey JS, Koh WJ, Evans ML, et al. Quantifying regional hypoxia in human tumors with positron emission tomography of [^{18}F]fluoromisonidazole: a pretherapy study of 37 patients. *Int J Radiat Oncol Biol Phys.* 1996;36:417–428.
3. Nehmeh SA, Lee NY, Schroder H, et al. Reproducibility of intratumor distribution of ^{18}F-fluoromisonidazole in head and neck cancer. *Int J Radiat Oncol Biol Phys.* 2008;70:235–242.
4. Thorwarth D, Alber M. Implementation of hypoxia imaging into treatment planning and delivery. *Radiother Oncol.* 2010;97:172–175.
5. Wang W, Georgi JC, Nehmeh SA, et al. Evaluation of a compartmental model for estimating tumor hypoxia via FMISO dynamic PET imaging. *Phys Med Biol.* 2009;54:3083–3099.
6. Oehler C, O'Donoghue JA, Russell J, et al. ^{18}F-fluromisonidazole PET imaging as a biomarker for the response to 5,6-dimethylxanthenone-4-acetic acid in colorectal xenograft tumors. *J Nucl Med.* 2011;52:437–444.
7. Krohn KA, Link JM, Mason RP. Molecular imaging of hypoxia. *J Nucl Med.* 2008;49(suppl 2):129S–148S.
8. Reischl G, Dorow DS, Cullinane C, et al. Imaging of tumor hypoxia with [^{124}I] IAZA in comparison with [^{18}F]FMISO and [^{18}F]FAZA: first small animal PET results. *J Pharm Pharm Sci.* 2007;10:203–211.
9. Postema EJ, McEwan AJ, Riauka TA, et al. Initial results of hypoxia imaging using 1-alpha-D: -(5-deoxy-5-[^{18}F]-fluoroarabinofuranosyl)-2-nitroimidazole (^{18}F-FAZA). *Eur J Nucl Med Mol Imaging.* 2009;36:1565–1573.
10. Fujibayashi Y, Taniuchi H, Yonekura Y, Ohtani H, Konishi J, Yokoyama A. Copper-62-ATSM: a new hypoxia imaging agent with high membrane permeability and low redox potential. *J Nucl Med.* 1997;38:1155–1160.
11. Holland JP, Lewis JS, Dehdashti F. Assessing tumor hypoxia by positron emission tomography with Cu-ATSM. *Q J Nucl Med Mol Imaging.* 2009;53:193–200.
12. Burgman P, O'Donoghue JA, Lewis JS, Welch MJ, Humm JL, Ling CC. Cell line-dependent differences in uptake and retention of the hypoxia-selective nuclear imaging agent Cu-ATSM. *Nucl Med Biol.* 2005;32:623–630.
13. O'Donoghue JA, Zanzonico P, Pugachev A, et al. Assessment of regional tumor hypoxia using ^{18}F-fluoromisonidazole and ^{64}Cu(II)-diacetyl-bis(N4-methylthiosemicarbazone) positron emission tomography: comparative study featuring microPET imaging, Po2 probe measurement, autoradiography, and fluorescent microscopy in the R3327-AT and FaDu rat tumor models. *Int J Radiat Oncol Biol Phys.* 2005;61:1493–1502.
14. Chia K, Fleming IN, Blower PJ. Hypoxia imaging with PET: which tracers and why? *Nucl Med Commun.* 2012;33:217–222.
15. Sharma R. Nitroimidazole radiopharmaceuticals in bioimaging: part I: synthesis and imaging applications. *Curr Radiopharm.* 2011;4:361–378.
16. Koch CJ, Scheuermann JS, Divgi C, et al. Biodistribution and dosimetry of ^{18}F-EF5 in cancer patients with preliminary comparison of ^{18}F-EF5 uptake versus EF5 binding in human glioblastoma. *Eur J Nucl Med Mol Imaging.* 2010;37:2048–2059.
17. Eskola O, Gronroos TJ, Forsback S, et al. Tracer level electrophilic synthesis and pharmacokinetics of the hypoxia tracer [^{18}F]EF5. *Mol Imaging Biol.* 2012;14:205–212.
18. van Loon J, Janssen MH, Ollers M, et al. PET imaging of hypoxia using [^{18}F] HX4: a phase I trial. *Eur J Nucl Med Mol Imaging.* 2010;37:1663–1668.
19. Dubois L, Landuyt W, Haustermans K, et al. Evaluation of hypoxia in an experimental rat tumour model by [^{18}F]fluoromisonidazole PET and immunohistochemistry. *Br J Cancer.* 2004;91:1947–1954.
20. Lehtio K, Oikonen V, Gronroos T, et al. Imaging of blood flow and hypoxia in head and neck cancer: initial evaluation with [^{15}O]H_2O and [^{18}F] fluoroerythronitroimidazole PET. *J Nucl Med.* 2001;42:1643–1652.
21. Li L, Hu M, Zhu H, Zhao W, Yang G, Yu J. Comparison of ^{18}F-fluoroerythronitroimidazole and ^{18}F-fluorodeoxyglucose positron emission tomography and prognostic value in locally advanced non-small-cell lung cancer. *Clin Lung Cancer.* 2010;11:335–340.
22. Yue J, Yang Y, Cabrera AR, et al. Measuring tumor hypoxia with ^{18}F-FETNIM PET in esophageal squamous cell carcinoma: a pilot clinical study. *Dis Esophagus.* 2012;25:54–61.
23. Vaupel P, Hockel M, Mayer A. Detection and characterization of tumor hypoxia using pO_2 histography. *Antioxid Redox Signal.* 2007;9:1221–1235.
24. Ling CC, Humm J, Larson S, et al. Towards multidimensional radiotherapy (MD-CRT): biological imaging and biological conformality. *Int J Radiat Oncol Biol Phys.* 2000;47:551–560.
25. Harada H. How can we overcome tumor hypoxia in radiation therapy? *J Radiat Res (Tokyo).* 2011;52:545–556.

JNM The Journal of NUCLEAR MEDICINE

PET of Hypoxia: Current and Future Perspectives

Sean Carlin and John L. Humm

J Nucl Med. 2012;53:1171-1174.
Published online: July 12, 2012.
Doi: 10.2967/jnumed.111.099770

The Journal of Nuclear Medicine is published monthly.
SNMMI | Society of Nuclear Medicine and Molecular Imaging
1850 Samuel Morse Drive, Reston, VA 20190.
(Print ISSN: 0161-5505, Online ISSN: 2159-662X)

SNMMI SOCIETY OF NUCLEAR MEDICINE AND MOLECULAR IMAGING